Altered platelet lipidome in bleeding patients with unexplained platelet function defects

Bianca de Jonckheere,[1,2*] Dino Mehic,[3,4*] Dominik Kopczynski,[1] Anita Pirabe,[3] Waltraud Schrottmaier,[3] Anna Schmuckenschlager,[3] Cristina Coman,[1] Tim Dreier,[4] Helmuth Haslacher,[5] Alexander Tolios,[6] Cihan Ay,[4] Ingrid Pabinger,[4] Johanna Gebhart,[4] Robert Ahrends[1#] and Alice Assinger[3#]

[1]Institute of Analytical Chemistry, University of Vienna; [2]Vienna Doctoral School in Chemistry, University of Vienna; [3]Institute of Vascular Biology and Thrombosis Research, Center of Physiology and Pharmacology, Medical University of Vienna; [4]Clinical Division of Hematology and Hemostaseology, Department of Medicine I, Medical University of Vienna; [5]Department of Laboratory Medicine, Medical University of Vienna and [6]Department of Transfusion Medicine and Cell Therapy, Medical University of Vienna, Vienna, Austria

BdJ and DM contributed equally as first authors.
RA and AA contributed equally as senior authors.

Correspondence: R. Ahrends
robert.ahrends@univie.ac.at

Received: February 26, 2025.
Accepted: July 14, 2025.
Early view: July 24, 2025.

https://doi.org/10.3324/haematol.2025.287698

Abstract

In patients with a mild to moderate bleeding disorder (MBD) and abnormal light transmission aggregometry (LTA), a platelet function defect (PFD) is suspected. However, in many patients with PFD, the underlying mechanism remains elusive. Given the essential role of lipids in platelet signaling, platelet lipid profiles in MBD patients with unexplained PFD may provide valuable diagnostic and mechanistic insights. This prospective cohort study investigated platelet lipidomes in patients with PFD of unknown cause from the Vienna Bleeding Biobank (VIBB). Using a standardized lipidomics workflow, we analyzed platelets from 27 patients and 19 age- and sex-matched controls and found that sex-specific lipid shifts emerged exclusively within the patient cohort, with greater deviations in females. Furthermore, lipid alterations correlated with impaired platelet aggregation and were predictive of responses to ADP and TRAP-6 stimuli in LTA experiments. Baseline and stimulated platelet analyses in a female subgroup showed intrinsic lipidomic changes, including upregulated polyunsaturated triacylglycerols (PUFA-TG), acylcarnitines (CAR), and reduced lysophosphatidylethanolamines (LPE). This study emphasizes lipidomic profiling as a promising diagnostic tool for unexplained platelet dysfunction and highlights TG, CAR, and LPE as potential therapeutic targets. Further research into lipid-driven platelet regulation may advance personalized treatments and improve clinical outcomes for patients with MBD.

Introduction

Cardiovascular disease remains the leading cause of death in the aging population,[1] where vascular imbalance exacerbates both thrombosis and bleeding risks, with notable sex differences in disease progression.[2,3] Although significant advancements have been made in thrombosis risk assessment and management, bleeding complications remain a critical, timely, and major clinical issue.

Patients with mild to moderate bleeding disorders (MBD), exhibiting symptoms such as epistaxis, easy bruising, or heavy menstrual bleeding frequently present at tertiary centers for a diagnostic work-up.[4,5] Their risk of bleeding increases during hemostatic challenges such as trauma, surgery, or childbirth, where bleeding can even be life-threatening.[6,7] Many of these cases involve an unknown cause of bleeding,[8] highlighting the urgent need for better diagnostic tools and a deeper understanding of bleeding pathophysiology to improve risk assessment and treatment options.

The Vienna Bleeding Biobank (VIBB) is a prospective, single-center cohort study that systematically enrolls bleeding patients without a prior diagnosis of a bleeding disorder since 2009.[8] These patients have undergone extensive testing for coagulation disorders and platelet function defects (PFD). In some patients with MBD, a PFD is suspected due to abnormalities observed in light transmission aggregometry (LTA), degranulation, and/or impaired glycoprotein expression.[8,9] However, unlike severe PFD such as Glanzmann thrombasthenia or Bernard-Soulier syndrome, the mechanisms underlying impaired platelet reactivity in these

patients remain poorly understood.[9] Pathological genetic variants are only identified in a quarter of patients with PFD.[10] This highlights the limitations of current diagnostic tools and a notable lack of targeted treatment options for MBD, particularly in high-risk hemostatic situations.

Platelets are vital in maintaining hemostasis and preventing excessive bleeding after vascular injury. Complex signaling pathways, which include lipid-mediated mechanisms,[11-13] are essential to platelet function, influencing key processes such as activation, aggregation, and interactions with the coagulation cascade. Upon platelet activation, alterations in the platelet lipid membrane composition result in the production of lipid messengers[13,14] and redistribution of phospholipids between the plasma membrane leaflets,[15] thereby enhancing coagulation factor binding.[16] Dysregulation of these processes can lead to hyperactive or hypoactive platelet responses, increasing the risk of thrombosis or bleeding, respectively. Moreover, lipids serve as highly sensitive biomarkers[17] and changes in their profiles often precede other molecular events.[18] Given the critical role of lipids in platelet physiology and function, investigating the platelet lipidome offers a promising approach to understanding bleeding tendencies, such as those linked to PFD.

This study aims to investigate the platelet lipidome in a well-defined subgroup of PFD patients with an undefined mechanism recruited from the VIBB cohort. It compares platelet lipid profiles in their resting state and after activation with thrombin receptor-activating peptide 6 (TRAP-6), providing novel insights into lipid-related mechanisms underlying platelet dysfunction.

Methods

Patient cohort

Patients from the VIBB and healthy controls from the Vienna bleeding study (VIBS) were analyzed. Inclusion and exclusion criteria were published previously[9] and are summarized in *Online Supplementary Table S1*. Participants underwent broad hemostatic investigations, as shown in *Online Supplementary Table S2*. Both the VIBB (EC no. 603/2009) and VIBS (EC no. 039/2006) have been approved by the Ethics Committee of the Medical University Vienna according to the Declaration of Helsinki of 1975. All study participants signed a written informed consent.

Investigated patients

This sub-study included 27 bleeding patients with unexplained PFD, identified through clinical routine diagnostics, based on abnormal LTA (N=25), reduced glycoprotein VI expression (N=1), or decreased P-selectin expression (N=1). Patients were compared to 19 age- and sex-matched healthy controls without a clinically relevant bleeding tendency. Patients and controls were invited for one or two follow-up investigations, where blood was drawn for further analyses (see below).

Blood draw

Blood samples were collected under fasting conditions via antecubital venipuncture using a 21-gauge butterfly needle (Greiner Bio-One, Kremsmuenster, Austria) into Vacuette tubes (Greiner Bio-One, Kremsmuenster, Austria), with processing occurring within 1 hour of collection.

Light transmission aggregometry

To platelet-rich plasma (PRP) in an optical 4-channel aggregometer, ADP (14 μM) or TRAP-6 (15 μM) was added to record changes in light transmission over 10 minutes (min). A detailed description is provided in the *Online Supplementary Appendix*.

Platelet isolation and stimulation

Washed platelets were frozen immediately (basal) or stimulated with 20 μM TRAP-6 for 5 min and then frozen at -80°C until further analysis. Isolation and stimulation protocols are described in detail in the *Online Supplementary Appendix*.

Lipid extraction

Platelet samples were processed using the SIMPLEX procedure described elsewhere.[19] Dried lipid fractions were resuspended for further mass spectrometry (MS) analysis. Internal lipid standards for quantification were added prior to extraction. A detailed description of the extraction procedure and standards is reported in the *Online Supplementary Appendix*.

Lipid analysis

Shotgun lipidomic analysis was performed using a TriVersa Nanomate coupled to an Orbitrap mass spectrometer. Acquired spectra were analyzed using LipidXplorer.[20] MS acquisition and data analysis parameters are detailed in the *Online Supplementary Appendix*. Workflow details are also provided in the ILS Reporting Checklist (*Online Supplementary Appendix*).

Identification of shared features by LipidSpace

LipidSpace[21] was employed for the comparison of basal platelet lipidomes by utilizing pairwise structural similarity metrics and quantitative data. A detailed description can be found in the *Online Supplementary Appendix*.

Statistical analysis

Statistical analysis was done with R (v4.3.2)/R-Studio (v2023.09.1.494). Variables are presented as means with standard deviations. Boxplot boundaries represent the 25th and 75th percentile, the center line the median, and whiskers extend from the hinge to the largest or smallest value no further than 1.5x the interquartile range (IQR). Two-group comparisons of normal distributed data was

analyzed using a two-sided Student's *t* test or Welch's *t* test (unequal sample sizes). For non-normal distributions, a Wilcoxon rank sum test was employed. ANOVA was used for multiple groups. *P* values less than 0.05 were considered significant (*$P \leq 0.05$; **$P \leq 0.01$; ***$P \leq 0.001$).

Results

Clinical and laboratory characteristics

Clinical and laboratory characteristics of patients and age- and sex-matched healthy controls are shown in Table 1. At study inclusion, patients had a median bleeding score (ISTH-BAT) and number of bleeding manifestations of 6.5 (IQR, 4.0-9.0) and 3.0 (IQR, 2.0-5.0), respectively. A family history of bleeding was reported by 63% of patients. No differences in platelet count, immature platelet fraction, or coagulation parameters were observed. Patients had slightly lower factor (F) VIII levels, albeit within the normal range in all patients. Notably, patients had a significantly longer closure time in the platelet function analyzer (PFA-100), indicating impaired platelet function.

Quantitative assessment of the platelet lipidome

The lipid composition of human platelets was quantitatively analyzed using a robust and standardized lipidomics workflow (Figure 1A). In a first step, platelets were frozen immediately after processing to preserve the lipidome under basal conditions. Lipid profiles were obtained using the two-phase extraction method following the SIMPLEX protocol[19] and shotgun lipidomics via direct infusion tandem mass spectrometry (MS/MS). This approach enabled the detection and quantification of 17 distinct lipid classes across four major lipid categories. In addition, the comparative analyses revealed no significant differences in the lipid profiles of male and female healthy control subgroups, except for lysophosphatidylethanolamine (LPE), which was less abundant in males (Figure 1B, C; *Online Supplemen-*

Table 1. Clinical and laboratory characteristics of patients and healthy controls.

Characteristics	Patients N=27	Healthy controls N=19	*P*
	N (%)	N (%)	
Positive family history of bleeding	16 (59)	0 (0)	<0.001
Female sex	17 (63)	12 (63)	0.989
	Median (IQR)	Median (IQR)	
Age, years	38.0 (31.0-43.0)	35.0 (25.0-40.0)	0.326
Vicenza bleeding score	5.0 (4.0-8.0)	-	NA
ISTH-BAT bleeding score	6.5 (4.0-9.0)	-	NA
N of bleeding manifestations	3.0 (2.0-5.0)	-	NA
Hemoglobin, g/dL	14.0 (13.2-15.1)	13.8 (13.0-14.5)	0.525
Platelets, $x10^9$/L	250.0 (204.0-284.0)	264.0 (222.0-298.0)	0.265
Immature platelet fraction*, $x10^9$/L	8.6 (7.1-11.5)	10.3 (7.6-15.6)	0.362
Immature platelet fraction*, %	3.3 (2.7-6.1)	3.8 (3.0-6.2)	0.505
Mean platelet volume*, fL	10.5 (10.1-11.0)	10.8 (10.0-11.2)	0.285
Prothrombin time, %	89.0 (82.0-95.0)	89.0 (81.5-94.0)	0.729
APTT, seconds	36.7 (35.2-39.3)	35.0 (33.5-38.1)	0.103
Fibrinogen, mg/dL	287.0 (252.0-342.0)	277.0 (248.0-329.0)	0.428
FVIII, %	98.0 (84.0-129.0)	127.0 (110.0-144.0)	0.028
FIX, %	86.0 (80.0-102.0)	86.0 (81.0-98.0)	0.902
FXIII*, %	134.5 (121.0-186.0)	143.0 (119.0-154.0)	0.713
PFA-100 (epinephrine), seconds	164.0 (132.0-189.0)	122.0 (103.0-149.0)	<0.001
VWF:Ag, %	95.0 (72.0-114.0)	102.0 (92.0-115.0)	0.088
VWF:Act, %	94.0 (78.0-136.0)	113.0 (98.0-146.0)	0.160

*Missing values: immature platelet fraction in 5 patients and 1 healthy control, mean platelet volume in 1 patient, FXIII in 1 patient. IQR: interquartile range (25^{th}, 75^{th} percentile); NA: not applicable; ISTH-BAT: International Society on Thrombosis and Hemostasis bleeding assessment; APTT: activated partial thromboplastin time; VWF: von Willebrand factors; Ag: antigen; Act: activity; F: factor.

tary Figure S1A). However, few notable differences were observed at the lipid class level, with more significant deviations detected within the female patient cohort. The highest inter-donor variation in lipid concentrations was found in sterol lipids, specifically cholesterol esters (SE) and cholesterol (ST), as well as in triacylglycerols (TG). Apart from a modest increase in phosphatidylcholine (PC) and cardiolipin (CL) levels in menopausal patients, menopausal status did not significantly alter the platelet lipidome in either healthy controls or patients (*Online Supplementary Figure S1B*).

Evaluation of the lipidome similarity and cohort-specific variability

Next, we employed LipidSpace,[21] an advanced tool for analyzing lipidomes based on structural and quantitative features, to explore platelet lipidome similarities and cohort-specific variability. LipidSpace enables the comparison of lipidomes by utilizing pairwise structural similarity metrics and quantitative data. Hierarchical clustering of the lipidomes revealed good separation for most samples, with an accuracy of 87% (Figure 2A, B). Furthermore, two distinct clusters, luster 1 and luster 2, emerged as the most divergent from the control groups. Interestingly, 11 of the 12 patients from these clusters were females.

Principal component analysis (PCA) was used to visualize the lipidomic data in a reduced dimensional space, considering lipid quantities (Figure 2C). The analysis revealed tight clustering of control and patient samples, with most data points grouped closely within the principal component space. However, a few patients (6, 10, and 11) are positioned significantly further from the main clusters, particularly along the first principal component, indicating more significant individual lipidomic differences.

Z-score normalization of the selected lipid species (Figure 2D) revealed that patient groups exhibited higher lipid concentration variability than controls, particularly among male patients. Female patients displayed a noticeable upward shift in lipid concentration compared to sex-matched controls, while male patients exhibited broader heterogeneity in their lipid profiles. The 34 lipids contributing most significantly to the cohort separation were distributed across nine lipid classes (Figure 2E). Statistically significant differences were observed in less abundant lipid classes, such as lysophosphatidylcholine (LPC) and LPE. Both bioactive lipids are significantly downregulated in female patients compared to the sex-matched control group.

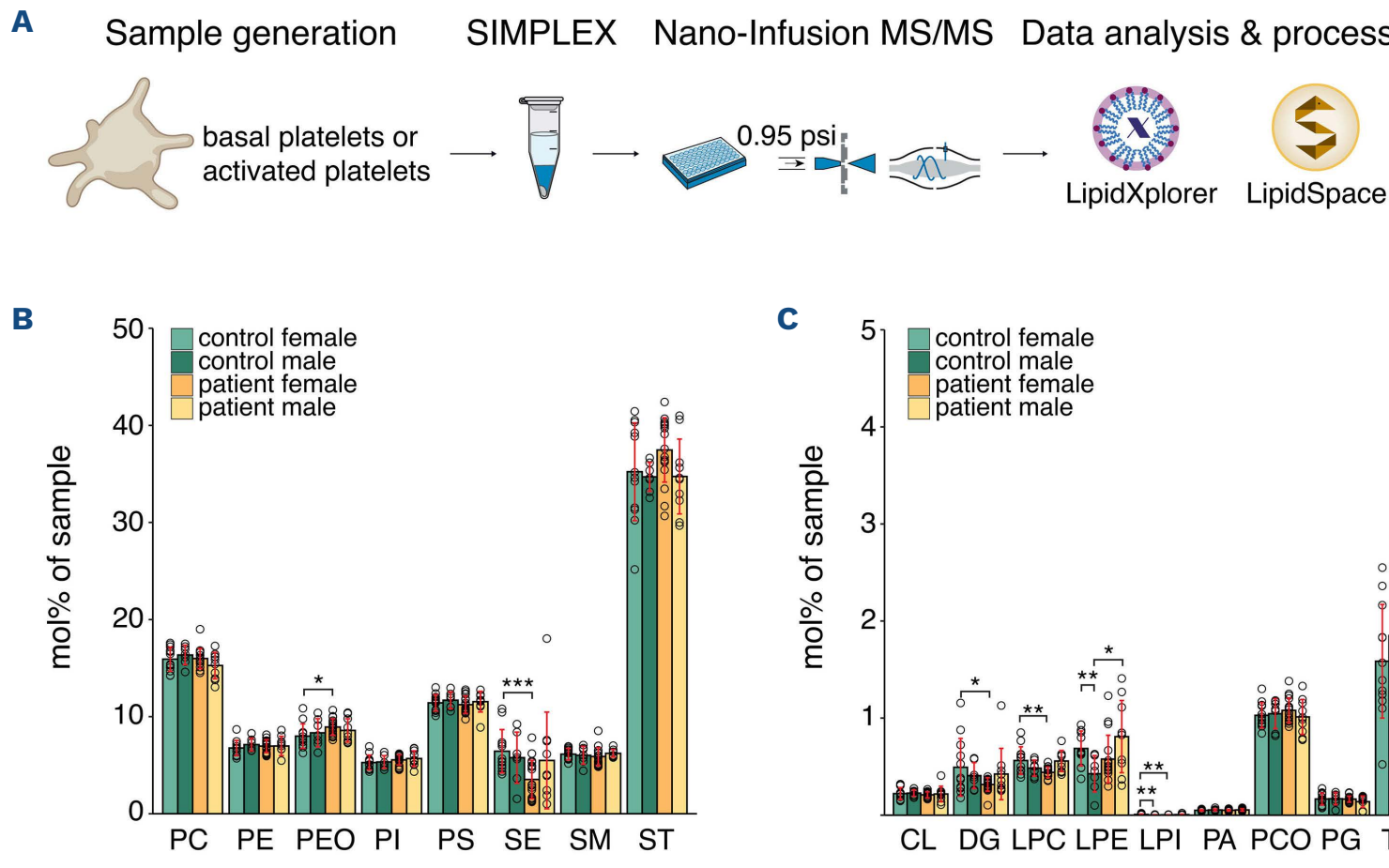

Figure 1. Lipidomics workflow and lipid class distribution in control and patient groups. (A) The lipidomics workflow includes sample generation, lipid extraction, measurement via high-resolution mass spectrometry, and subsequent data analysis and processing. (B) Mean relative abundance of high-abundance lipid classes across control and patient groups, separated by biological sex. (C) Relative abundance of low-abundance lipid classes, shown for the same groups as in (B). A two-sided *t* test was performed to compare control subgroups and sex-matched groups statistically. Comparison of patient subgroups was not considered. Each data point represents 1 donor (control female [N=12], control male [N=7], patient female [N=17], patient male [N=10]). PC: phosphatidylcholine; PE: phosphatidylethanolamine; PEO: PE-ether; PI: phosphatidylinositol; PS: phosphatidylserine; SE: cholesterol ester; SM: sphingomyelin; ST: cholesterol; CL: cardiolipin; DG: diacylglycerol; LPC: lyso-PC; LPE: lyso-PE; LPI: lyso-PI; PA: phosphatidic acid; PCO: PC-ether; PG: phosphatidylglycerol; TG: triacylglycerol. *$P \leq 0.05$; **$P \leq 0.01$; ***$P \leq 0.001$.

Association of selected lipid species with light transmission aggregometry data

Next, we wanted to link the lipidomic and clinical data to get valuable insight into the correlation between lipid changes and global hemostatic platelet capacity. Therefore, LTA data from donors obtained parallel to platelet sample

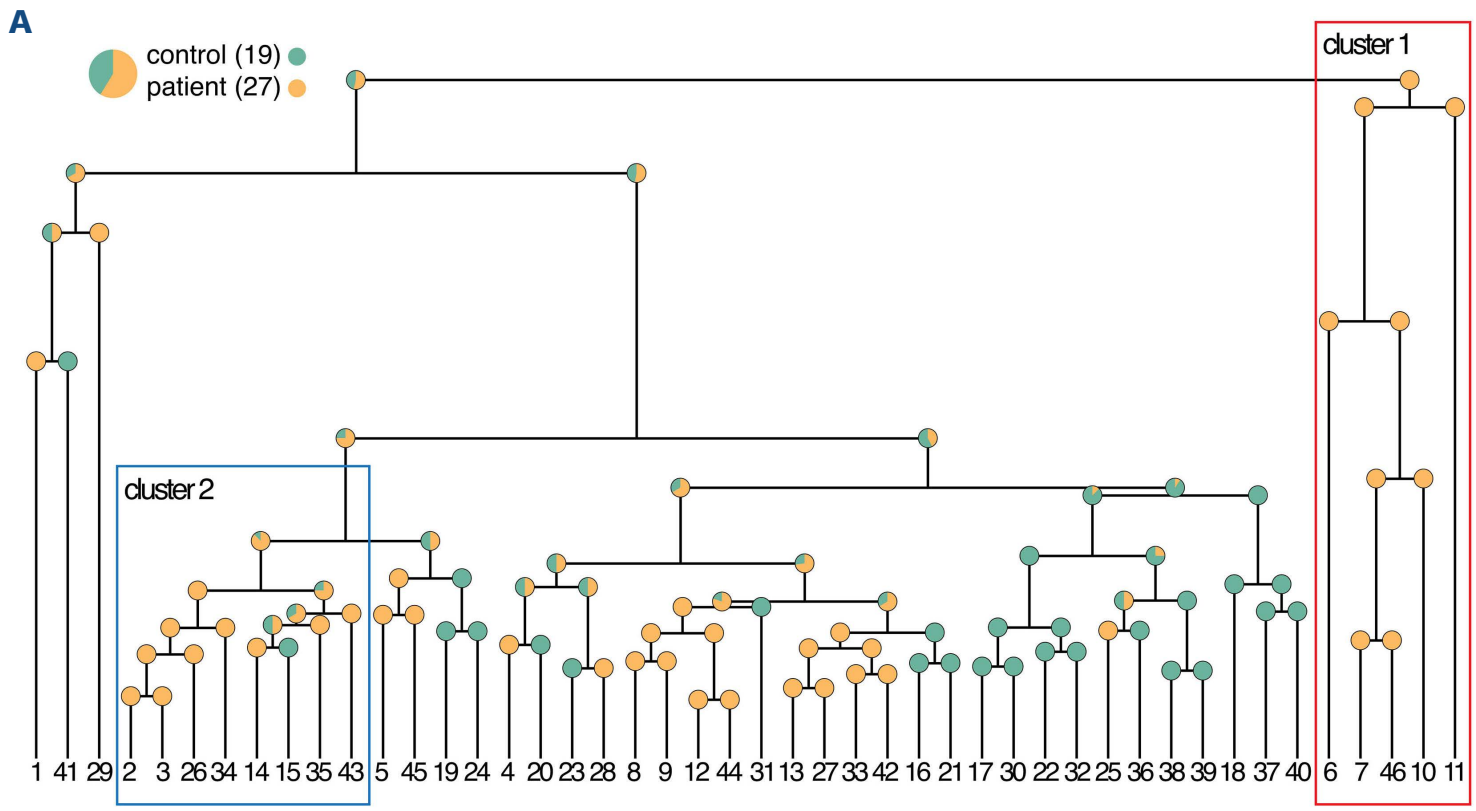

Figure 2. Cohort-based lipid feature analysis reveals separation between control and patient groups, with a stronger effect in females. (A) Dendrogram illustrating separation of control and patient groups after cohort-based feature analysis using LipidSpace, based on chemical space clustering of selected lipid species. Two distinct clusters (cluster 1 [red] and 2 [blue]) were identified with high dissimilarity to controls. (B) Classification accuracy of cohort separation using lipid occurrence data and Z-scoring of lipid concentrations. (C) Principal component analysis shows a distinct separation of control and patient groups. Patient ID from clusters 1 and 2 are highlighted and color-coded according to (A). (D) Statistical comparison of Z-scores of selected lipid species by ANOVA across control and patient subgroups. (E) The distribution of selected lipid species from cohort-based feature analysis is displayed as lipid classes. Each data point represents one donor (control female [N=12], control male [N=7], patient female [N=17], patient male [N=10]). CL: cardiolipin; DG: diacylglycerol; LPC: lyso-PC; LPE: lyso-PE; PA: phosphatidic acid; PC: phosphatidylcholine; PCO: PC-ether; PE: phosphatidylethanolamine; PEO: PE-ether. *P<=0.05; **P<=0.01.

collection were linked to the results from the cohort-based feature analysis from LipidSpace. The selected lipid species were used to predict the area under the aggregometry curve (AUC) values from the LTA data. Measured AUC values for ADP (Figure 3A-C) and TRAP-6 (Figure 3D-F) stimuli, correlated strongly with the lipid-estimated AUC values in a linear regression analysis, with R^2=0.820 and R^2=0.812, respectively. Patients exhibited significantly lower AUC values than controls across both stimuli (Figure 3B, E), indicating reduced platelet aggregation capacity in the patient cohort. Notably, many patients belonging to the clusters identified in Figure 2A, with the most distinct and distant lipid profiles, also had the most reduced aggregation responses to platelet activation agents in LTA (Figure 3A, D). The cohort separation accuracy of approximately 70%, as indicated by AUC values derived from lipid occurrences, further reinforces the link between lipidomic profiles and platelet function.

In-depth analysis of basal and activated platelet lipidomes from cluster patients

Given the high similarity observed in the lipidomes of basal platelets across donors, we aimed to evaluate shared and distinct features between patient platelet lipidomes upon activation. Therefore, we conducted follow-up investigations analyzing basal and activated platelets from patients in clusters 1 and 2, as their platelet lipidomes were most distinct. Five of twelve patients (patients 2, 3, 6, 43, and 46), all female, accepted our invitation, and age- and sex-matched controls were included for comparison (Figure 4A). No differences in clinical characteristics, waist-hip

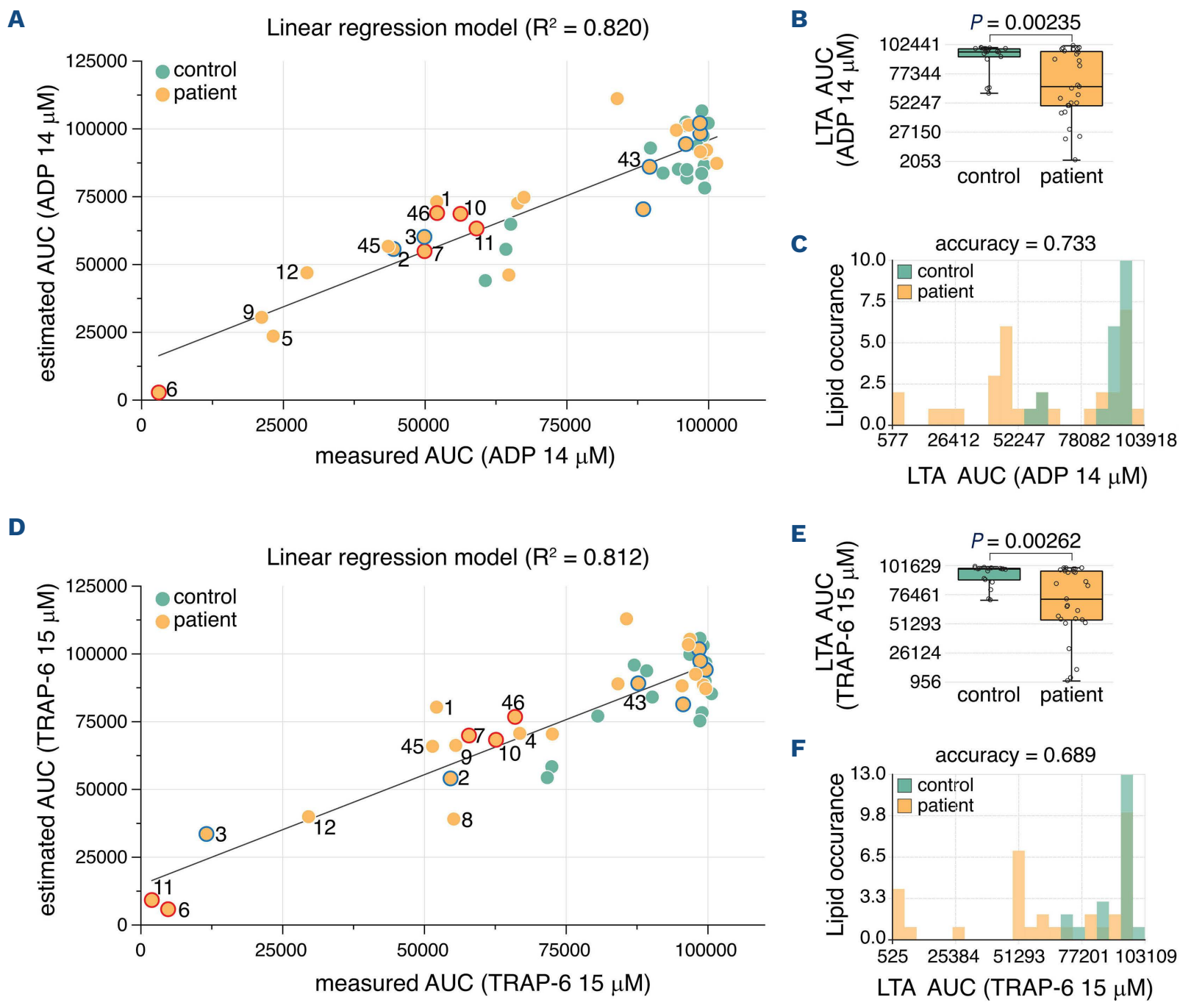

Figure 3. Linear regression analysis reveals a strong correlation between lipid-estimated and measured AUC values from platelet aggregation tests. (A) ADP linear regression model correlating measured and lipid-estimated AUC values from light-transmission aggregometry (LTA) experiments using 14 μM ADP as the platelet activation agent. (B) Statistical significance of the regression model determined by a two-sided *t* test. (C) Model accuracy for ADP-induced aggregation. (D, F) TRAP-6 linear regression analysis of platelet aggregation responses using 15 μM TRAP-6 as the activation agent, with (E) statistical significance evaluated by a two-sided *t* test and (F) model accuracy. Each data point represents one donor. Red and blue-circled points indicate cluster 1 and cluster 2 patients, respectively.

ratio, platelet count, coagulation parameters, lipid levels, or hormone levels were found between patients and controls (Table 2). This time, the experimental workflow, as outlined in Figure 1A, was adapted to include an additional step of activating platelets for 5 min with TRAP-6. This thrombin receptor agonist acts via the protease-activated receptor 1 (PAR1) pathway. Upon platelet activation, a distinct lipid signature could be observed for healthy controls (Figure 4B). Significantly regulated lipid species mostly belonged to the glycerophospholipids (GP, N=25), and only a few to either fatty acyls (FA, N=2), glycerolipids (GL, N=2), or sterol lipids (ST, N=1). Upregulated lipids that met the $\log_2$ fold change (FC) cutoff of +0.5 include lysophosphatidylinositols (LPI), LPE, and phosphatidic acids (PA), with the strongest FC observed for LPI 18:0 and LPI 18:1. Downregulated lipids ($\log_2$ FC cutoff -0.5) include acylcarnitines (CAR) 18:1 and 18:2, and lysophosphatidylglycerol (LPG) 22:6, along with notable downregulation of high-abundant phosphatidylinositol (PI) lipids, although with less pronounced FC. A complete list of the regulated lipid species is provided in the *Online Supplementary Table S3*.

To examine TRAP-6-specific lipid regulation in patients, we visualized the FC (TRAP-6/basal) in a heatmap (Figure 4C). Most patients (P2, P3, P6, and P46) exhibited similar trends in lipid regulation to those observed in controls. However, patient 43 showed minimal lipidomic response to TRAP-6 activation, with negligible regulation of upregulated and downregulated lipid species. Patient 6 also showed a reduced upregulation of LPE species, particularly LPE 16:0, LPE 17:0, and LPE 20:1, suggesting a muted response in this specific lipid class.

A broader analysis of all regulated lipid species across patients revealed additional differences compared to controls (Figure 4D). Patients exhibited not only shared regulatory patterns with controls but also distinct variations. Most notably, patient 43 demonstrated an overall lack of lipid regulation, with minimal changes across all lipid classes, corroborating the limited activation seen in Figure 4C. Patient 6 also exhibited fewer upregulated

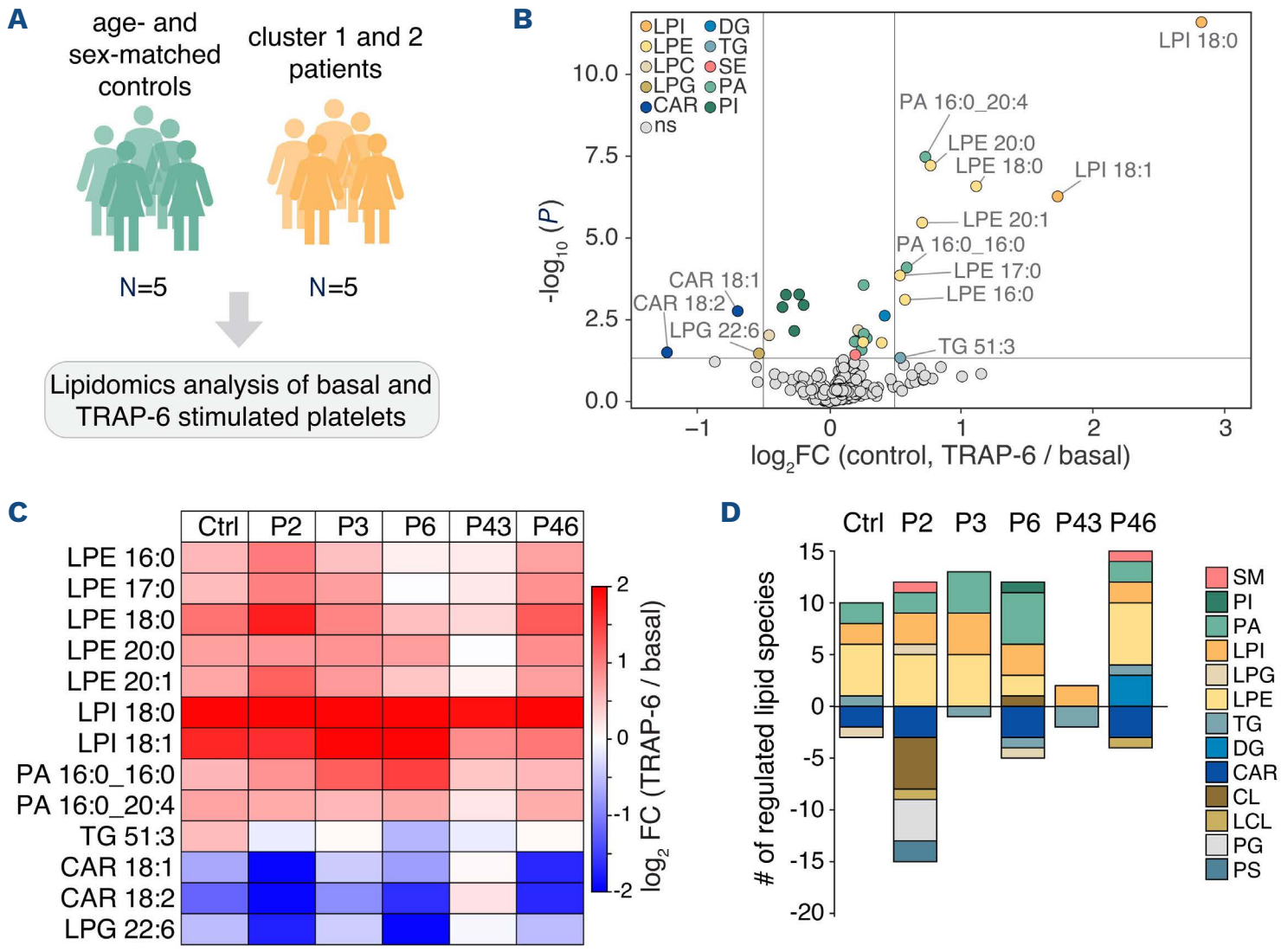

Figure 4. Platelet activation response and lipid regulation upon TRAP-6 stimulation. (A) Illustration of the study cohorts for platelet activation experiments using 20 μM TRAP-6. Five female patients from selected clusters are compared to 5 age- and sex-matched controls. (B) Volcano plot showing TRAP-6-specific lipid regulation in healthy controls, comparing basal *versus* TRAP-6-stimulated platelets. Significantly regulated lipid species are color-coded by lipid class, with lipid species exhibiting a $\log_2$ fold change (FC) above ±0.5 labeled. (C) Matrix of significantly regulated lipid species identified in activated control platelets ($\log_2$ FC cutoff ±0.5) showing their corresponding $\log_2$ FC values comparing basal and TRAP-6-stimulated platelets for controls (mean of 5 individuals) and individual patients (P2, P3, P6, P43, P46). (D) Bar graph illustrating the number of regulated lipid species ($\log_2$ FC cutoff ±0.5) per lipid class for controls and individual patients. NS: not significant; LPI: lyso-PI; LPE: lyso-PE; LPC: lyso-PC; LPG: lyso-PG; CAR: acylcarnitine; DG: diacylglycerol; TG: triacylglycerol; SE: cholesterol ester; PA: phosphatidic acid; PI: phosphatidylinositol; SM: sphingomyelin; CL: cardiolipin; LCL: lyso-CL; PG: phosphatidylglycerol; PS: phosphatidylserine.

species in the LPE class, consistent with the muted response highlighted earlier. Intriguingly, patient 2 showed pronounced downregulation of lipid classes related to energy metabolism, such as CL, lysocardiolipins (LCL), and phosphatidylglycerol (PG), which may reflect broader metabolic disturbances or mitochondrial dysfunction.

Intrinsic lipidomic alterations in basal and TRAP-6-stimulated platelets

To better understand the lipidomic differences between patients and controls, we compared the baseline lipid levels in both basal and TRAP-6-stimulated platelets, extending the analysis beyond activation-dependent lipid regulation. TRAP-6 was selected for its robust platelet activation and the significant reduction of P-selectin (CD62P) surface expression and procaspase activating compound-1 (PAC1) binding observed in patients (*Online Supplementary Figure S2*). Volcano plots were generated to visualize the differences in the patient cohort compared to controls, revealing distinct species-specific alterations (Figure 5A, B; *Online Supplementary Table S4*). Most prominently and most consistently, polyunsaturated triacylglycerols (PUFA-TG), such as TG 56:6, TG 56:7, TG 56:8, and TG 58:7, TG 58:8, TG 58:9, were upregulated in patients. Similarly, acylcarnitines, including CAR 16:0, CAR 18:1, and CAR 18:2, showed a significant upregulation in basal and activated platelets. Additionally, two ether-linked phosphatidylethanolamine species (PE O-17:1/22:6, PE O-16:1/22:6) were also found to be upregulated in patients

Table 2. Clinical and laboratory characteristics of patients and healthy controls at follow-up investigations.

Characteristics	Patients N=5	Healthy controls N=5	*P*
	N (%)	N (%)	
Female sex	5 (100)	5 (100)	>0.999
Family history of bleeding	2 (40)	0 (0)	0.444
	Median (IQR)	Median (IQR)	
Age, years	53.0 (45.0-57.0)	40.0 (37.0-42.0)	0.346
Waist-hip-ratio	0.7 (0.7-0.8)	0.8 (0.8-1.1)	0.063
Hemoglobin, g/dL	13.2 (12.6-13.7)	13.2 (13.1-13.4)	0.730
Platelets, x10^9/L	210.0 (187.0-248.5)	238.0 (234.0-248.0)	0.413
Immature platelet fraction*, x10^9/L	7.6 (5.3-9.4)	11.2 (10.2-11.9)	0.063
Immature platelet fraction*, %	5.1 (3.6-10.5)	4.5 (3.5-6.2)	>0.999
Prothrombin time, %	84.0 (81.0-95.0)	88.0 (84.0-100.0)	0.346
APTT, sec	35.1 (33.7-35.7)	35.2 (33.8-39.5)	>0.999
FVIII, %	121.0 (115.0-146.0)	112.0 (80.0-119.0)	0.222
FIX, %	87.0 (84.0-105.0)	90.0 (78.0-109.0)	0.675
FXIII, %	149.0 (145.0-166.0)	133.0 (131.0-187.0)	0.841
Triglycerides, mg/dL	78.0 (60.0-78.0)	69.0 (52.0-99.0)	0.834
Cholesterol, mg/dL	218.0 (208.0-220.0)	186.0 (182.0-192.0)	0.222
HDL, mg/dL	73.0 (63.0-79.0)	62.0 (59.0-96.0)	>0.999
LDL, mg/dL	123.0 (121.8-123.4)	110.2 (69.8-113.2)	0.310
Apolipoprotein A1, mg/dL	158.0 (150.0-170.0)	155.0 (144.0-167.0)	0.841
Apolipoprotein B, mg/dL	92.0 (87.0-102.0)	86.0 (57.0-94.0)	0.402
Lipoprotein (A), nmol/L	7.0 (7.0-17.0)	7.0 (7.0-7.0)	0.441
TSH, μIU/mL	1.3 (1.3-1.4)	1.8 (1.7-2.5)	0.421
Testosterone, ng/mL	0.2 (0.1-0.2)	0.1 (0.1-0.2)	>0.999
17-β-Oestradiol, pg/mL	6.0 (5.0-11.0)	70.0 (52.0-130.0)	0.094
Vitamin D, nmol/L	81.2 (57.0-83.7)	70.7 (65.2-72.0)	0.841
Vitamin B12, pmol/L	420.0 (167.0-538.5)	443.0 (343.0-491.0)	0.905

TSH: thyroid stimulating hormone; F: factor; APTT: activated partial thromboplastin time.

with high statistical significance.

On the other hand, patients had significantly downregulated TG species with a lower degree of saturation. Among the phospholipids, LPE 22:3 was consistently reduced in the patient group. Importantly, these lipid trends can be observed in basal and TRAP-6-stimulated platelets, suggesting that the underlying differences in lipid composition are intrinsic to the patient cohort and are not solely a result of platelet activation.

To investigate these trends further, we analyzed the degree of fatty acid saturation within TG. Although TG were not uniformly regulated on class level (Figure 5C), species-level analysis (Figure 5D) revealed a significant upregulation of PUFA in patients, alongside marked downregulation of saturated and monounsaturated FA. TG were classified as PUFA-TG if they contained four or more double bonds,

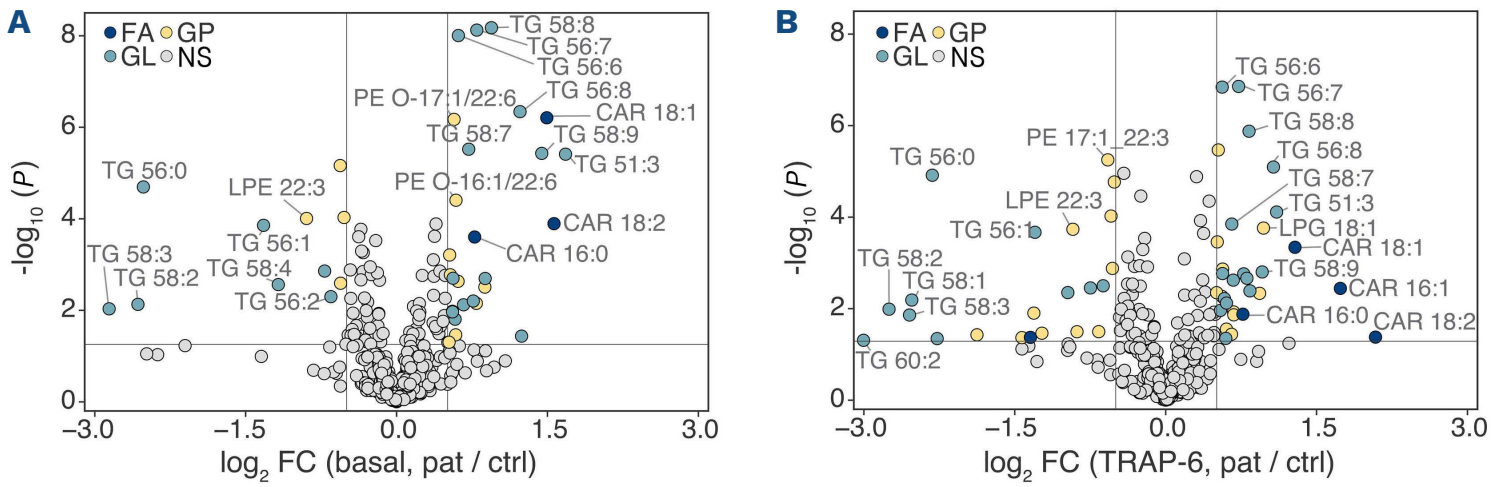

Figure 5. Comparative lipidomics analysis of basal and activated platelets in patients *versus* controls highlights distinct lipid signatures in patients. (A, B) Volcano plots comparing lipid abundances between patients and controls in (A) basal and (B) TRAP-6-activated platelets. Significantly regulated lipid species with a $\log_2$ fold change (FC) cutoff ±0.5 are shown, with color-coding based on lipid categories. (C) Triacylglycerol (TG) analysis at the lipid class level. (D) Bubble chart showing the degree of saturation of TG at the species level. The size of each bubble represents the mean lipid abundance in TRAP-6-stimulated platelets, with color indicating the $\log_2$ FC between patients and controls of stimulated platelets. (E) Acylcarnitine (CAR) analysis at the lipid class level. (F) Regulation of selected acylcarnitine species, focusing on upregulated species in patients. Data points represent replicates (N=4-6) from 5 donors per group. NS: not significant; FA: fatty acyl; GL: glycerolipids; GP: glycerophospholipid. *P≤0.05; **P≤0.01; ***P≤0.001.

though species with fewer double bonds may also qualify if combined with saturated fatty acids. However, due to identification on the species level, precise identification of fatty acid combinations was not possible.
CAR showed consistent upregulation at the class level (Figure 5E), with several species contributing to this trend in both basal and TRAP-6-stimulated platelets from patients (Figure 5F). Interestingly, upregulated platelet CAR species did not correlate with plasmatic coagulation factor activity in either patients or controls (*Online Supplementary Figure S3*), and corresponding plasma CAR levels remained unchanged (*Online Supplementary Figure S4*).

Platelet lipidome heterogeneity in the patient cohort

Besides the mutual trends in TG and CAR lipid classes, the analysis of the patient lipidomes also revealed considerable heterogeneity in some individuals with a unique lipidomic profile compared to the broader cohort trends. We performed hierarchical clustering based on Pearson's correlation of the mean lipid abundances in basal platelets (Figure 6A; *Online Supplementary Figure S5*). We identified patient 6 (P6) as the most divergent, indicating lipid regulation patterns markedly different from other patients. Visualizing the $\log_2$ FC in a heatmap, comparing individual patient lipid class levels to the control group for both basal and TRAP-6-stimulated platelets, we could observe lower lipid class concentrations for lysophosphatidic acid (LPA), LPE, PA, phosphatidylcholine-ether (PCO), PG, and phosphatidylserine (PS), and higher SE levels in most patients compared to controls. In contrast, patient 6 exhibited mostly opposite trends (Figure 6B). The heterogeneity of the patient's platelet lipidomes can mask significant lipid trends, as shown exemplarily for LPA, LPE, PA, and PS, lipid classes critical for platelet activation (Figure 6C), where distinct differences in lipid abundance between controls, the patient cohort excluding patient 6 (pat#), and patient 6 can be observed.
Interestingly, while most patients showed a similar activation pattern of LPE species during TRAP-6-mediated platelet activation, we observed significantly lower levels of LPE 16:1, LPE 18:1, LPE 18:3, LPE 20:1, LPE 20:3, LPE 20:5, LPE 22:1, LPE 22:3, and LPE 22:4 in the patient cohort excluding patient 6 compared to controls (Figure 6D), which seem independent of phospholipase C (PLC) activity (*Online Supplementary Figure S6*). LPE 18:1 and LPE 20:1 were upregulated during activation in healthy controls, and lower levels (Figure 6E) might have reduced the platelet activation potential in the patients. Notably, although total LPE was significantly upregulated in patient 6 compared to controls and other patients, LPE 22:3 and LPE 22:4 were consistently downregulated in all patients (Figure 6F).

Discussion

In this study, we used state-of-the-art high-resolution mass spectrometry to explore the platelet lipidome of patients with a mild-to-moderate bleeding tendency and a suspected PFD of unknown cause. Despite exhibiting platelet counts and immature platelet fractions comparable to healthy controls, these patients showed mild to severe platelet aggregation defects in LTA analysis. While few studies recently emerged exploring the platelet lipidome during a state of infection or inflammation,[22-25] the platelet lipidome of patients with hereditary PFD thus far has remained unexplored.
This study reveals three key findings. First, female patients demonstrated greater deviation in their basal platelet lipid profiles than males, suggesting potential sex-specific influences on lipid metabolism in disease states. Second, platelet activation via the PAR1 receptor triggered similar lipid responses in patients and healthy controls, indicating that fundamental aspects of platelet activation remain preserved despite platelet function defects. Lastly, distinct platelet lipidomic signatures are linked to platelet function, providing a foundation for future research into lipid markers for improved diagnosis and personalized therapeutic strategies.
Our lipidomic analysis of resting platelets aligns closely with previously reported lipid class profiles of human platelets,[26,27] though we observed higher SE concentrations, consistent with findings by Cebo *et al.*[28] and Ruebsaamen *et al.*[29] In line with the literature, we also observed no differences in most lipid classes in basal platelets in sex-mixed healthy controls.[26] However, significant sex-specific differences emerged exclusively within the patient cohort, with greater deviations in females, suggesting that sex-specific biological processes, such as hormonal regulation, immune response, or metabolic adjustments, may be activated or altered due to the pathological condition. Sex differences exist in susceptibility to and progression of various cardiovascular diseases,[30-32] including MBD.[2]
The most notable lipid level differences between patients and controls were found in CAR, TG, and LPE, all from low-abundance classes. Additionally, the summed concentrations of the 34 lipids contributing to the cohort separation in LipidSpace accounted for less than 10 mol%, indicating that changes within abundant platelet lipids were minimal while emphasizing subtle, disease-related lipidomic alterations.
We found a significant increase in acylcarnitines in female patients with PFD. CAR might function as anticoagulant lipids by inhibiting plasmatic coagulation factor binding.[33] Previously, acylcarnitines were associated with increased bleeding risk in patients with coronary artery disease (CAD) and even showed predictive potential for mortality or recurring myocardial infarction in CAD patients.[22,25,34] Our findings underline CAR as metabolic regulators in platelets and suggest that their altered abundance may contribute to the bleeding phenotype observed in PFD. Although CAR accumulated primarily within platelets and not in plasma,

reflecting platelet-intrinsic metabolic dysregulation, we cannot exclude potential local effects on coagulation factors, particularly in the microenvironment of platelet activation. Functional assays or analyses based on coagulation factor purification are needed to determine the bioavailability and binding status of CAR (free *vs.* factor-bound), which may influence their functional relevance and are not captured by standard lipidomics sample preparation.

Furthermore, we observed that the alterations in TG levels in patients with PFD may be influenced, at least in part, by the saturation degree of the lipid species. While the precise causes and functional consequences of these changes remain speculative, the shifts in TG and CAR levels among female PFD patients suggest a potential impact on platelet

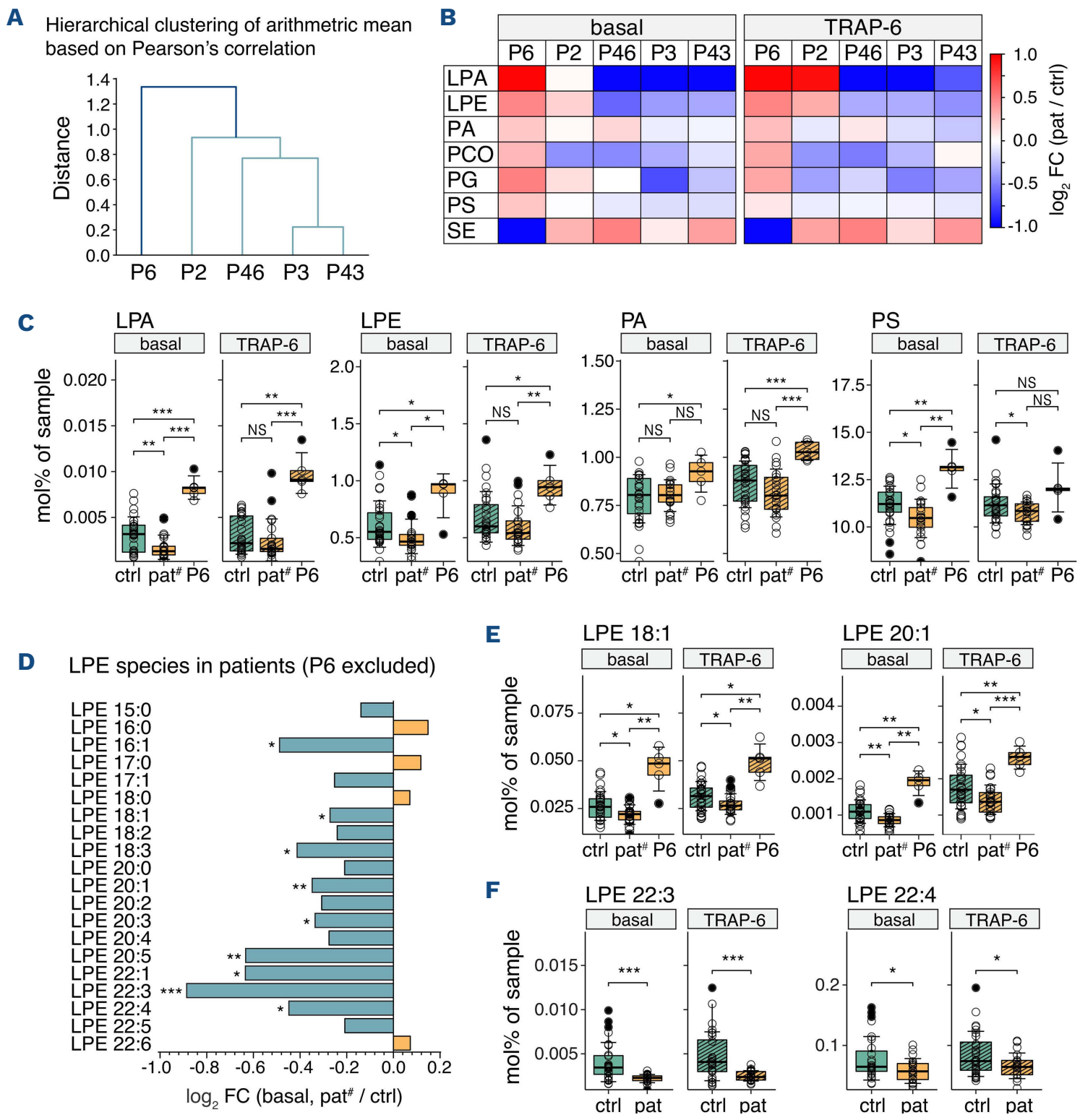

Figure 6. Patient heterogeneity obscures significant lipid trends, highlighting unique lipid profiles in individual cases. (A) Hierarchical clustering of the mean lipid abundances in basal platelets, based on Pearson's correlation, shows patient 6 (P6) as the most distinct from other patients. (B) Heatmap illustrating lipid classes with opposite regulation trends in patient 6 compared to other patients, with prominent lipid classes displayed as a matrix of log_2 fold changes (FC) (patient *vs.* control) for basal and TRAP-6-stimulated platelets. Colors represent log_2 FC values. (C) Selected lipid classes critical for platelet activation, showing differences in lipid abundance at the class level in controls, patients excluding patient 6 (pat#, N=4), and patient 6, for both basal and TRAP-6-stimulated platelets. (D) Patients excluding patient 6 show significantly lower LPE species levels than controls (representative basal levels shown). Asterisks indicate significance. (E) LPE species upregulated during TRAP-6-induced platelet activation. (F) LPE species showing significantly lower levels in all patients and consistent lipid regulation across the patient cohort. Data points represent replicates (N=4-6) from 5 donors per group. NS: not significant; LPA: lyso-PA; LPE: lyso-PE; PA: phosphatidic acid; PCO: PC-ether; PG: phosphatidylglycerol; PS: phosphatidylserine; SE: cholesterol ester. *P≤0.05; **P≤0.01; ***P≤ 0.001.

fatty acid metabolism. TG serve as energy reservoirs, mobilized through lipolysis to fuel mitochondrial β-oxidation, a process facilitated by CAR, which shuttle long-chain fatty acids into mitochondria for oxidative phosphorylation. Elevated levels of CAR and PUFA-TG observed in these patients could suggest impaired β-oxidation. Platelets rely on β-oxidation of fatty acids to generate the energy required for structural and functional changes during activation.[35,36] As fatty acid metabolism follows distinct pathways driven by enzyme selectivity for chain length and degree of saturation,[37] the characteristic TG profile may reflect a shift in mitochondrial energy metabolism or selective lipid utilization within platelets. Consistently, these findings align with the growing evidence that alterations in fatty acid availability and processing can influence platelet functionality and energy homeostasis.[38]

However, the lower LPE levels are most interesting. Decreased LPE levels in our patient cohort align with studies linking LPE to altered platelet activation thresholds.[39] Furthermore, elevated platelet LPE levels have previously been associated with increased cardiovascular risk,[22] supporting our findings of reduced LPE levels in patients with bleeding tendencies. The LPE reduction could potentially impair the MAPK/ERK1/2 pathway, whose activation goes hand in hand with platelet functions such as thromboxane A2 release and thrombus formation.[40] While a potential upstream role of PLC in regulating LPE levels was considered, the lack of significant differences in PLC activity or linear relationship to LPE levels suggest that altered LPE dynamics in PFD patients are likely governed by PLC-independent mechanisms. Nonetheless, the dependency of the MAPK/ERK1/2 pathway on LPE levels has yet to be established in platelets and warrants further mechanistic investigation.[41-43]

The current study highlights several critical considerations in the investigation of lipidomic changes associated with PFD. For dietary-sensitive lipids such as TG, diet is a relevant factor to consider. Although dietary intake was not explicitly controlled for, the lack of significant differences in waist-hip ratio (Table 2) minimizes the likelihood of major dietary discrepancies. Notably, the distinct lipid pattern persists despite the high inter-donor variation ($CV_{patients}$>38.4%) within the TG class.

Furthermore, while the small sample size limits the ability to define robust biomarkers, it offers valuable insights that could guide future research in the right direction. To achieve more comprehensive and reliable conclusions, investigations of larger cohorts are warranted. However, this poses practical challenges, as PFD of unknown causes is rare, even within the VIBB, one of the largest clinical biobanks for MBD. Immediate next steps should include expanding the current findings to the full study cohort while incorporating male participants to explore sex-specific similarities or differences. Longitudinal analyses could also be instrumental in tracking LPE changes over time and under hemostatic challenges, providing a dynamic perspective on disease progression and response to stimuli. Further, while TRAP-6 was used as a potent activator of the PAR-1 pathway in this study, it is important to acknowledge that different agonists, such as ADP, epinephrine, or collagen, trigger distinct platelet signaling pathways and may lead to unique lipidomic responses. A broader evaluation using multiple agonists could help differentiate between receptor-specific and shared lipid regulation patterns and fully elucidate the complexity of platelet lipid signaling in PFD. Ultimately, these efforts may guide the development of targeted therapeutic strategies to restore lipid homeostasis in PFD patients and offer a promising path for improving patient outcomes.

In conclusion, we report distinctive lipidomic changes in platelets from patients with PFD compared to age- and sex-matched healthy controls. Further, we were able to link distinct lipid profiles to reduced aggregation responses to platelet activation agents *ex vivo*. These results highlight that lipidomic alterations can be linked to bleeding tendency.

Disclosures

DM received honoraria for advisory board meetings from CSL Behring and Sobi. CA received honoraria from Bayer, CSL Behring, Novo Nordisk, Pfizer, Roche, Sobi, and Takeda for lectures and/or participation in advisory board meetings. IP has received honoraria from Bayer, CSL Behring, Novo-Nordisk, Pfizer, Roche, Sobi, and Takeda for lectures and advisory board meetings. JG received honoraria for lectures and advisory board meetings and research funding for the Medical University of Vienna from CSL Behring, Novartis, Amgen, Sobi, and Takeda. All other authors have no conflicts of interest to disclose.

Contributions

BdJ conducted the lipidomics experiments, analyzed data, generated the figures, and wrote the initial draft of the manuscript. DM recruited patients, performed experiments, analyzed data, and critically revised the manuscript. DK analyzed data. AP, WS, AS, and CC helped with experiments. TD recruited patients. HH coordinated biobanking. AT supervised routine platelet function testing. CA, IP, and JG recruited patients and established the prospective cohort study. RA and AA developed the concept, coordinated the project, and critically revised the manuscript. All authors read and approved the final manuscript.

Acknowledgments

We gratefully acknowledge the support provided by the Mass Spectrometry Centre (MSC) at the Faculty of Chemistry, University of Vienna.

Funding

The Vienna Bleeding Biobank was supported by the Anniversary Fund of the Austrian National Bank (grant number 18500), an unrestricted grant of CSL Behring and the medical-scientific fund of the Mayor of the federal capital

Vienna (grant number 20023). DM received the Physician Pathway Scholarship of the Medical University of Vienna for protected research time. The authors received support from the University of Vienna through seed funding and funding derived from the Vienna Doctoral School in Chemistry (DoSChem) at the Faculty of Chemistry, University of Vienna (RA). The study was funded by the Austrian Science Fund (FWF) P-32064, P-34783, and I6303-B.

Data-sharing statement

Data supporting the findings of this study are available in the Online Supplementary Appendix. Raw data are available on reasonable request from the corresponding author.

References

1. Eurostat. Causes of death - monthly statistics. 2024. Available from: https://ec.europa.eu/eurostat. Accessed January 17, 2025.
2. Atiq F, Saes JL, Punt MC, et al. Major differences in clinical presentation, diagnosis and management of men and women with autosomal inherited bleeding disorders. EClinicalMedicine. 2021;32:100726.
3. Shufelt CL, Pacheco C, Tweet MS, Miller VM. Sex-specific physiology and cardiovascular disease. Adv Exp Med Biol. 2018;1065:433-454.
4. Rodeghiero F, Pabinger I, Ragni M, et al. Fundamentals for a systematic approach to mild and moderate inherited bleeding disorders: an EHA consensus report. Hemasphere. 2019;3(4):e286.
5. Mezzano D, Quiroga T. Diagnostic challenges of inherited mild bleeding disorders: a bait for poorly explored clinical and basic research. J Thromb Haemost. 2019;17(2):257-270.
6. Rossaint R, Afshari A, Bouillon B, et al. The European guideline on management of major bleeding and coagulopathy following trauma: sixth edition. Crit Care. 2023;27(1):80.
7. Bienstock JL, Eke AC, Hueppchen NA. Postpartum hemorrhage. N Engl J Med. 2021;384(17):1635-1645.
8. Gebhart J, Hofer S, Panzer S, et al. High proportion of patients with bleeding of unknown cause in persons with a mild-to-moderate bleeding tendency: results from the Vienna Bleeding Biobank (VIBB). Haemophilia. 2018;24(3):405-413.
9. Mehic D, Gebhart J, Pabinger I. Bleeding disorder of unknown cause: a diagnosis of exclusion. Hamostaseologie. 2024;44(4):287-297.
10. Downes K, Megy K, Duarte D, et al. Diagnostic high-throughput sequencing of 2396 patients with bleeding, thrombotic, and platelet disorders. Blood. 2019;134(23):2082-2091.
11. Manke M-C, Ahrends R, Borst O. Platelet lipid metabolism in vascular thrombo-inflammation. Pharmacol Ther. 2022;237:108258.
12. Manke MC, Geue S, Coman C, et al. ANXA7 Regulates platelet lipid metabolism and Ca(2+) release in arterial thrombosis. Circ Res. 2021;129(4):494-507.
13. Peng B, Geue S, Coman C, et al. Identification of key lipids critical for platelet activation by comprehensive analysis of the platelet lipidome. Blood. 2018;132(5):e1-e12.
14. Rubenzucker S, Manke M-C, Lehmann R, Assinger A, Borst O, Ahrends R. A Targeted, bioinert LC–MS/MS method for sensitive, comprehensive analysis of signaling lipids. Anal Chem. 2024;96(23):9643-9652.
15. Clark SR, Thomas CP, Hammond VJ, et al. Characterization of platelet aminophospholipid externalization reveals fatty acids as molecular determinants that regulate coagulation. Proc Natl Acad Sci U S A. 2013;110(15):5875-5880.
16. Heemskerk JWM, Bevers EM, Lindhout T. Platelet activation and blood coagulation. Thromb Haemost. 2002;88(08):186-193.
17. Laaksonen R, Ekroos K, Sysi-Aho M, et al. Plasma ceramides predict cardiovascular death in patients with stable coronary artery disease and acute coronary syndromes beyond LDL-cholesterol. Eur Heart J. 2016;37(25):1967-1976.
18. Ekroos K, Lavrynenko O, Titz B, Pater C, Hoeng J, Ivanov NV. Lipid-based biomarkers for CVD, COPD, and aging - A translational perspective. Prog Lipid Res. 2020;78:101030.
19. Coman C, Solari FA, Hentschel A, Sickmann A, Zahedi RP, Ahrends R. Simultaneous metabolite, protein, lipid extraction (SIMPLEX): a combinatorial multimolecular omics approach for systems biology. Mol Cell Proteomics. 2016;15(4):1453-1466.
20. Herzog R, Schuhmann K, Schwudke D, et al. LipidXplorer: a software for consensual cross-platform lipidomics. PLoS One. 2012;7(1):e29851.
21. Kopczynski D, Hoffmann N, Troppmair N, et al. LipidSpace: simple exploration, reanalysis, and quality control of large-scale lipidomics studies. Anal Chem. 2023;95(41):15236-15244.
22. Harm T, Dittrich K, Brun A, et al. Large-scale lipidomics profiling reveals characteristic lipid signatures associated with an increased cardiovascular risk. Clin Res Cardiol. 2023;112(11):1664-1678.
23. Harm T, Bild A, Dittrich K, et al. Acute coronary syndrome is associated with a substantial change in the platelet lipidome. Cardiovasc Res. 2021;118(8):1904-1916.
24. Schuurman AR, Léopold V, Pereverzeva L, et al. The platelet lipidome is altered in patients with COVID-19 and correlates with platelet reactivity. Thromb Haemost. 2022;122(10):1683-1692.
25. Chatterjee M, Rath D, Schlotterbeck J, et al. Regulation of oxidized platelet lipidome: implications for coronary artery disease. Eur Heart J. 2017;38(25):1993-2005.
26. Heimerl S, Höring M, Kopczynski D, et al. Quantification of bulk lipid species in human platelets and their thrombin-induced release. Sci Rep. 2023;13(1):6154.
27. Leidl K, Liebisch G, Richter D, Schmitz G. Mass spectrometric analysis of lipid species of human circulating blood cells. Biochimica et Biophysica Acta (BBA) - molecular and cell biology of lipids. Biochim Biophys Acta. 2008;1781(10):655-664.
28. Cebo M, Calderón Castro C, Schlotterbeck J, Gawaz M, Chatterjee M, Lämmerhofer M. Untargeted UHPLC-ESI-QTOF-MS/MS analysis with targeted feature extraction at precursor and fragment level for profiling of the platelet lipidome with ex vivo thrombin-activation. J Pharm Biomed Anal. 2021;205:114301.
29. Ruebsaamen K, Liebisch G, Boettcher A, Schmitz G. Lipidomic analysis of platelet senescence. Transfusion. 2010;50(8):1665-1676.
30. Norris CM, Yip CYY, Nerenberg KA, et al. State of the science in women's cardiovascular disease: a Canadian perspective on the influence of sex and gender. J Am Heart Ass. 2020;9(4):e015634.
31. Maas AHEM, Rosano G, Cifkova R, et al. Cardiovascular health after menopause transition, pregnancy disorders, and other gynaecologic conditions: a consensus document from European

cardiologists, gynaecologists, and endocrinologists. Eur Heart J. 2021;42(10):967-984.
32. Mehta LS, Beckie TM, DeVon HA, et al. Acute myocardial infarction in women. Circulation. 2016;133(9):916-947.
33. Deguchi H, Banerjee Y, Trauger S, et al. Acylcarnitines are anticoagulants that inhibit factor Xa and are reduced in venous thrombosis, based on metabolomics data. Blood. 2015;126(13):1595-1600.
34. Shah SH, Sun J-L, Stevens RD, et al. Baseline metabolomic profiles predict cardiovascular events in patients at risk for coronary artery disease. Am Heart J. 2012;163(5):844-850.e841.
35. Slatter DA, Aldrovandi M, O'Connor A, et al. Mapping the human platelet lipidome reveals cytosolic phospholipase A2 as a regulator of mitochondrial bioenergetics during activation. Cell Metab. 2016;23(5):930-944.
36. Ravi S, Chacko B, Sawada H, et al. Metabolic plasticity in resting and thrombin activated platelets. PLoS One. 2015;10(4):e0123597.
37. Han X. Lipidomics for studying metabolism. Nat Rev Endocrinol. 2016;12(11):668-679.
38. Kulkarni PP, Ekhlak M, Dash D. Energy metabolism in platelets fuels thrombus formation: halting the thrombosis engine with small-molecule modulators of platelet metabolism. Metabolism. 2023;145:155596.
39. Xiao H, Siddiqui RA, Al-Hassani M, Slíva D, Kovacs RJ. Phospholipids released from activated platelets improve platelet aggregation and endothelial cell migration. Platelets. 2001;12(3):163-170.
40. Flaumenhaft R. Stressed platelets ASK1 for a MAPK. Blood. 2017;129(9):1066-1068.
41. Makiyama F, Kawase S, Omi AW, et al. Differential effects of structurally different lysophosphatidylethanolamine species on proliferation and differentiation in pre-osteoblast MC3T3-E1 cells. Sci Rep. 2025;15(1):466.
42. Hisano K, Kawase S, Mimura T, et al. Structurally different lysophosphatidylethanolamine species stimulate neurite outgrowth in cultured cortical neurons via distinct G-protein-coupled receptors and signaling cascades. Biochem Biophys Res Commun 2021;534:179-185.
43. Park SJ, Lee KP, Im DS. Action and signaling of Lysophosphatidylethanolamine in MDA-MB-231 breast cancer cells. Biomol Ther (Seoul). 2014;22(2):129-135.